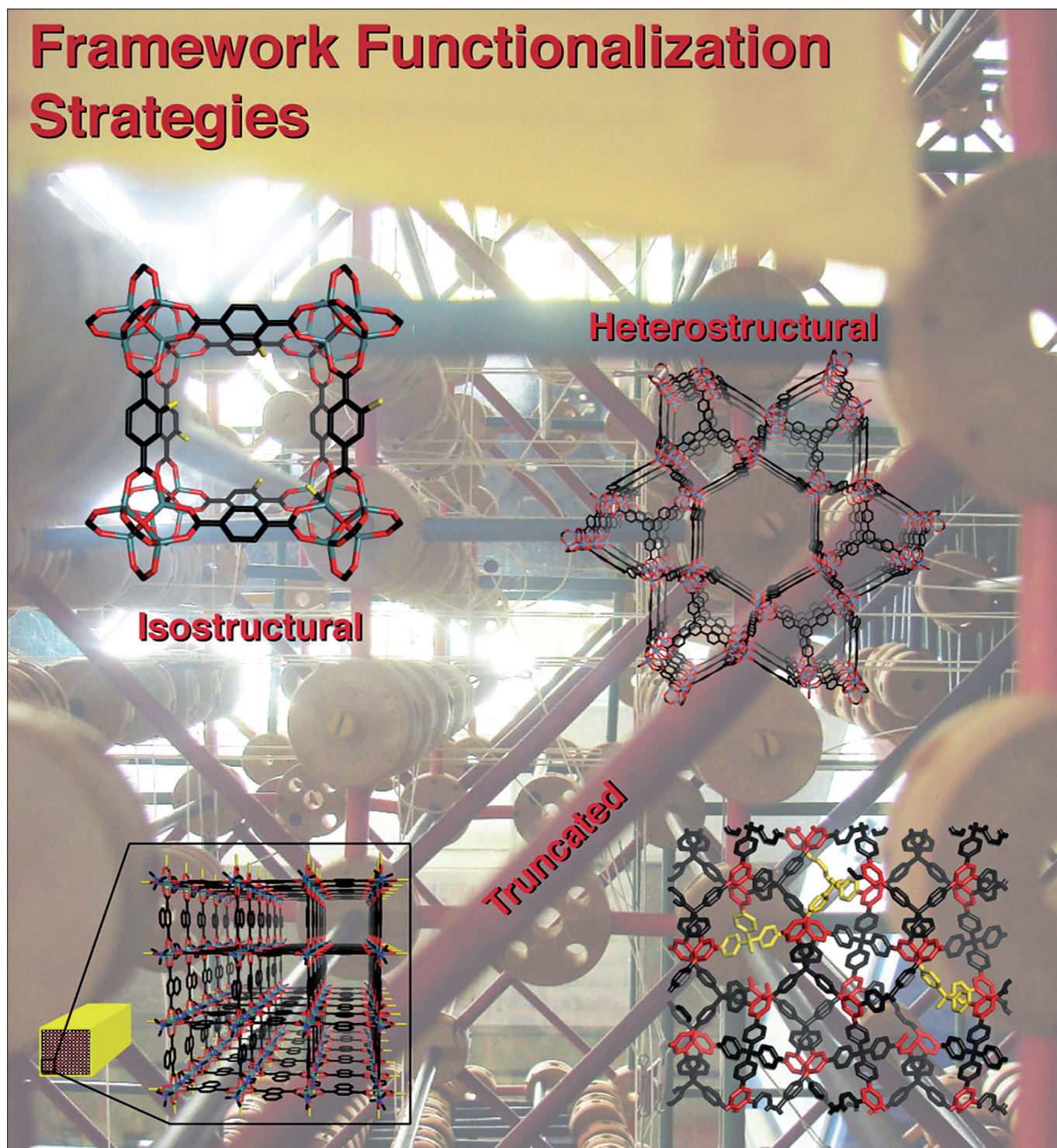


Mixed Linker Strategies for Organic Framework Functionalization

David N. Bunck and William R. Dichtel^{*,[a]}

Framework Functionalization Strategies



Abstract: Framework materials have attracted intense interest for gas storage, separations, catalysis, and other applications as a consequence of their periodicity, high specific surface area, and rational synthesis. Cocrystallizing multiple monomers with identical linking chemistry represents an emerging route to access materials with increased complexity and advanced functions. This Concept Article highlights three strategies for framework synthesis that employ mixtures of monomers with 1) identical linking geometries, 2) different linking geometries, or 3) in which one monomer is truncated with respect to the other. These approaches offer a diverse toolbox to modify framework topology, incorporate active functionality, and rationally control crystallite size and morphology.

Keywords: covalent organic frameworks • crystal engineering • functionalization • metal–organic frameworks • self-assembly

Introduction

Framework materials are a class of polymers whose structures impart unique properties distinct from other macromolecular architectures. These materials are defined by their periodicity and permanent porosity, which results in exceptionally large surface areas and makes them privileged for applications in separations, payload storage and release, and catalysis. Framework crystallization employs reversible reactions, which facilitate the correction of defects, loops, and dangling chain ends during the polymerization to furnish ordered macromolecules. These materials can be divided into two classes. Metal–organic frameworks^[1] (MOFs) contain organic subunits linked by coordination bonds, which are directed by metal ions or clusters known as secondary building units^[2] (SBUs). The diverse set of metal coordination bonds and geometries provides an infinite number of potential network topologies, with thousands of MOFs described thus far. Covalent organic frameworks^[3,4] (COFs) are an emerging class of framework materials linked by covalent bonds. These materials are mostly comprised of light elements such as C, B, O, and N. COFs employ linkages that are formed reversibly, including boronate esters,^[5] imines,^[6] and hydrazones,^[7] to yield either layered 2D sheets or 3D nets. The 2D materials exhibit high intrinsic charge mobilities of interest for optoelectronic and energy-storage devices,^[8] whereas 3D COFs exhibit exceptional surface areas ($>4000\text{ m}^2\text{ g}^{-1}$) and record low densities (0.17 g cm^{-3}).^[4,9]

The majority of MOFs and COFs are high-symmetry structures synthesized from the minimum number of monomers (usually 1–2) dictated by their linkage chemistry. However, employing multiple monomers provides an opportunity to access frameworks with new properties. Frameworks might be functionalized to improve their gas adsorption behavior, enable covalent attachment of molecular payloads, or to include active catalysts. In this Concept Article, we highlight three strategies for functionalizing framework materials by cocrystallizing mixtures of organic building blocks. These strategies are illustrated in Figure 1 for a cubic framework. The first and most straightforward method is an isostructural mixed linker (IML) approach, which involves mixing two or more monomers with identical linking geometry.^[10] The IML approach is often employed to incorporate reactive functionality along the walls of a framework. Alternatively, monomers bear different linkage geometries in a heterostructural mixed linker (HML) strategy. At some monomer feed ratios, the resulting framework distributes the minority component throughout a defective lattice of the majority component. However, certain ratios provide lower symmetry topologies that are less prone to forming interpenetrated structures. The last strategy employs a second monomer with a reduced number of functional groups, denoted as a truncated mixed linker (TML) approach. Here, the second monomer acts as a capping agent that, depending on the kinetics of framework crystallization, either directs crystallite morphology and surface chemistry or enables functionalization of the framework interior.

Isostructural Mixed Linker Approaches

Perhaps the most simple and versatile way to incorporate multiple monomers into framework materials is to crystallize them using two or more organic building blocks with identical size and linkage chemistry, denoted as an isostructural mixed linker (IML) approach.^[10,11] For example, combining two (or more) terephthalic acid derivatives yields the mixed-composition MOF-5 cubic framework (Figure 2). Mixing multiple isostructural monomers provides a simple means to change framework properties, such as surface area, pore volume, reactivity, sorbent selectivity, and loading capacity, by varying the identity and ratio of these building blocks. The IML strategy sometimes provides frameworks with emergent properties distinct from the corresponding single component MOFs, as has been demonstrated in several examples highlighted below.

To the best of our knowledge, Kim and co-workers were the first to employ the IML strategy when they incorporated a mixture of terephthalic acid (**1**) and tetramethylterephthalic acid (**2**) into the $[\text{Zn}_2(\mathbf{1})_2\text{dabco}]$ framework (Figure 2b).^[12] The two monomers were incorporated into the framework in a 1:1 ratio, matching their feed ratio, as determined by ¹H NMR spectroscopy of the digested MOF. Refinement of

[a] D. N. Bunck, Prof. Dr. W. R. Dichtel
Department of Chemistry and Chemical Biology
Cornell University, Baker Laboratory, Ithaca, NY 14853-1301 (USA)
E-mail: wdichtel@cornell.edu

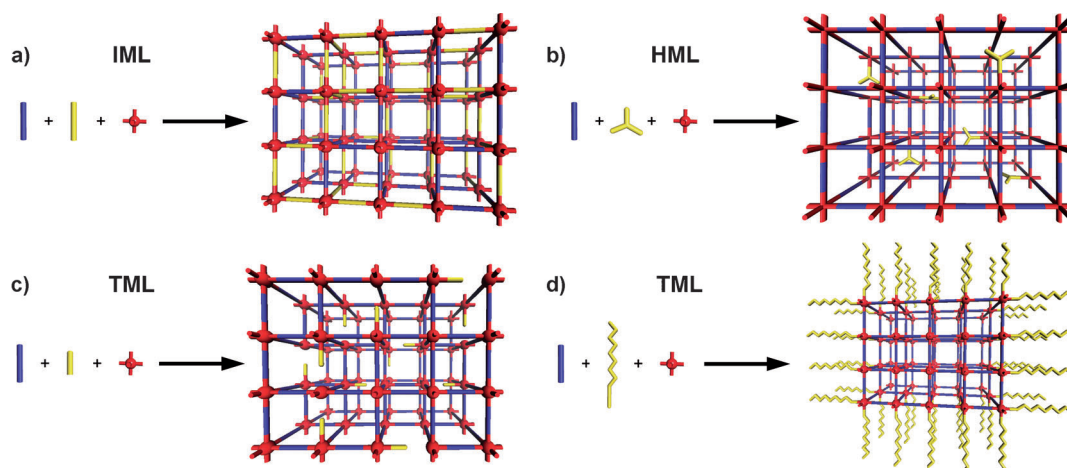


Figure 1. Illustrations of the a) isostructural mixed linker (IML), b) heterostructural mixed linker (HML), and c, d) two outcomes of truncated mixed linker (TML) approaches to framework functionalization.

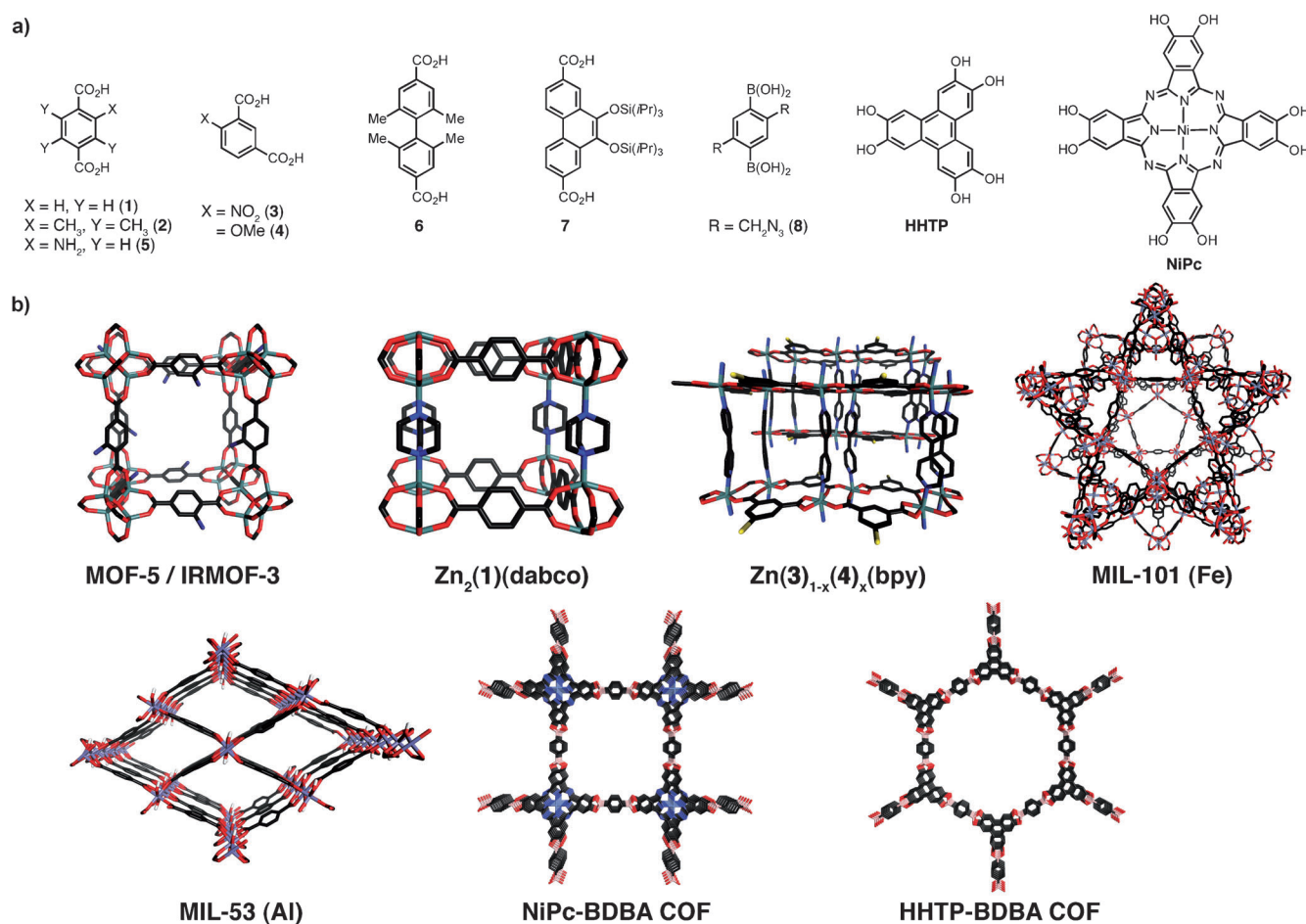


Figure 2. a) Monomers employed in the IML strategy with b) depictions of their corresponding frameworks.

the site occupancy factors for **1** and **2** derived from single-crystal X-ray diffraction data revealed equal contributions from each monomer throughout the framework, suggesting that they are distributed randomly throughout the MOF. Materials with increased fractions of **2** exhibited linear de-

creases in surface area over three data points (0, 50, and 100 mol% **2**). These data suggest that many framework properties of IML MOFs will scale linearly between those of MOFs derived from the individual linkers in the absence of cooperative effects.

Kitagawa and co-workers subsequently tuned pore flexibility across a series of MOFs containing varying ratios of 5-nitroisophthalic acid (**3**) and 5-methoxyisophthalic acid (**4**) within a $[\text{Zn}(\mathbf{3})_{1-x}(\mathbf{4})_x(\text{bpy})]$ network (Figure 2b).^[13] At ambient pressure, the pure $[\text{Zn}(\mathbf{4})(\text{bpy})]$ MOF adopts an open-pore structure and the $[\text{Zn}(\mathbf{3})(\text{bpy})]$ MOF is nonporous. However, $[\text{Zn}(\mathbf{3})(\text{bpy})]$ undergoes a nonporous to porous transition at a specific gate-opening pressure (P_{go}). Frameworks containing mixtures of **3** and **4** showed a tunable P_{go} for CO_2 adsorption, and a network containing 13% **4** ($x=0.13$) showed promise for separating CO_2 from CH_4 . In contrast, the permanently porous $[\text{Zn}(\mathbf{4})(\text{bpy})]$ MOF adsorbed CO_2 and CH_4 nonselectively.

Several studies have employed mixtures of terephthalic acids to load specific functionality into the pores of various frameworks, including MOF-5 (based on Zn),^[14] MIL-53 (Al),^[15,16] and MIL-101 (Fe)^[17] (Figure 2b). Baiker and co-workers characterized the thermal stability of amine-functionalized MOF-5 derivatives and used these amines both as nucleophilic catalysts^[18] and as ligands for Pd-catalyzed cross-coupling reactions.^[19] The authors also characterized the phase purity of mixed component frameworks using convenient thermogravimetric analysis (TGA) measurements.^[15] Cohen and co-workers incorporated amine- and bromoterephthalic acids into MOF-5 to demonstrate sequential and orthogonal reactions of these two groups, providing a means to prepare elaborate MOFs with multiple pendant functionalities.^[20] More recently, the same group obtained IML frameworks through postsynthetic ligand exchange, in which a second functionalized monomer was substituted into the intact framework.^[21] Lin and co-workers recently used the IML approach to load biologically relevant payloads into

MIL-101,^[17] including a fluorescent dye and a cisplatin pro-drug. HT-29 human colon adenocarcinoma cells show uptake of silica-coated, fluorescently labeled MIL-101- NH_2 nanoparticles, suggesting that such functionalized MOFs might be useful materials for bioimaging and drug-delivery applications.

Matzger and co-workers highlight another useful aspect of the IML approach using the MOF-5/IRMOF-3 system, in which a building block that crystallizes reliably is used to template the formation of a MOF whose monomers otherwise crystallize poorly.^[22] The authors identified conditions in which **5** and $\text{Zn}(\text{NO}_3)_2$ yield crystalline, high surface area IRMOF-3, but using **1** produces phase-impure, low surface area MOF-5. Cocrystallizing the two building blocks provided high surface area materials over a wide range of monomer ratios, even as low as 10% **5** (Figure 3a). Interestingly, this MOF also showed a higher surface area than even the pure IRMOF-3. While MOF-5 can be crystallized effectively under other conditions, this approach, if general, could streamline the empirical and often labor-intensive process of identifying growth conditions for new or poorly behaved building blocks.

The same report also describes an approach to suppress MOF interpenetration, in which one or more additional networks form within the pore volume of the first.^[22] This phenomenon arises from free volume effects, which often occur in highly symmetric networks containing long linkers. Interpenetrated MOFs typically exhibit decreased pore volume and surface area and increased density. For example, a framework formed exclusively from dicarboxylate **6** yields a doubly interpenetrated structure with a Brunauer–Emmett–Teller surface area ($S_{\text{BET-N}_2}$) of $1700 \text{ m}^2 \text{ g}^{-1}$. This surface

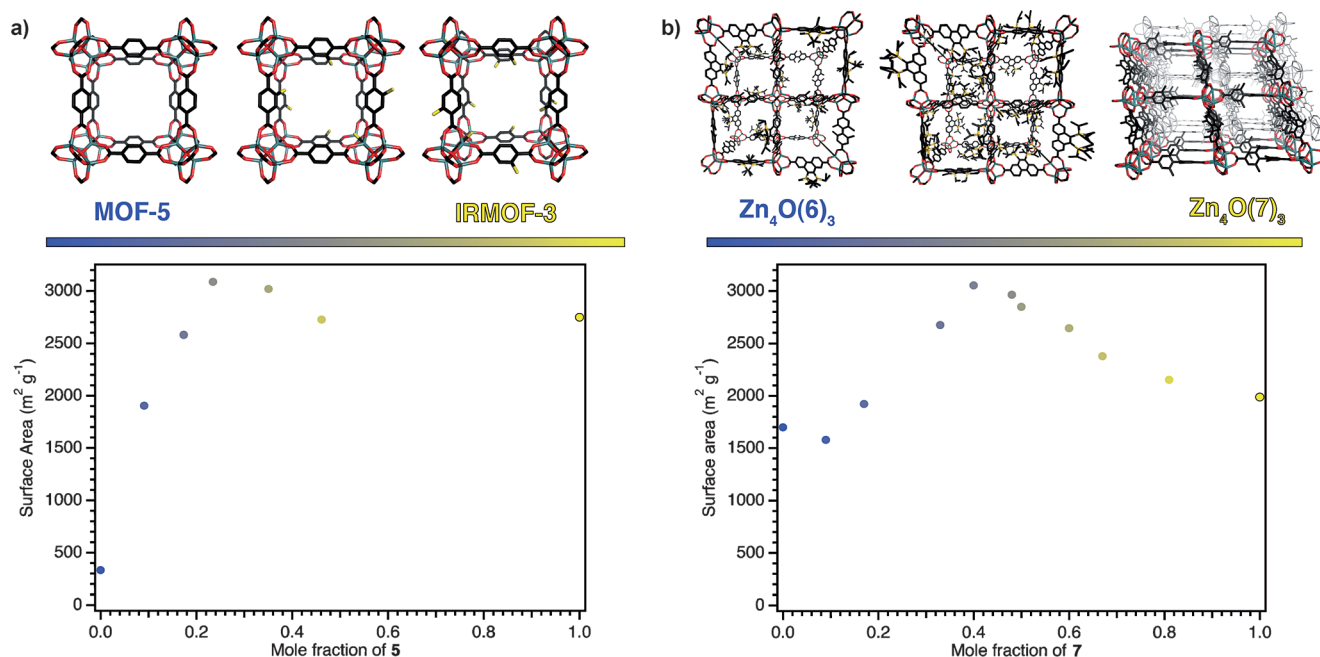


Figure 3. a) Cocondensation of **1** and **5** yield IML frameworks with higher surface area than either single-component framework. b) Incorporating **7** into MOFs composed of **6** prevents framework interpenetration and also provides increased surface area.

area increases as phenanthrene dicarboxylate **7** is incorporated into the material, up to $3000 \text{ m}^2 \text{ g}^{-1}$, at 40% **7** (Figure 3b). The powder X-ray diffraction patterns of the mixed composition MOFs indicated the preferential formation of noninterpenetrated cubic phases, although interpenetrated networks were also observed in many cases. This study demonstrates the utility of the IML approach for crystal engineering.

Yaghi and co-workers demonstrated the versatility of the IML strategy by preparing eighteen mixed-composition MOF-5 derivatives using nine substituted terephthalic acid building blocks.^[23] Nine of these MOFs were comprised of binary mixtures, while the other nine were ternary or higher order. Remarkably, two different ternary mixtures showed increased H_2 storage capacity and adsorption selectivity for CO_2 over CO . In separate work, Yaghi and co-workers used an IML approach to prepare MOFs linked by binary mixtures of imidazoles, often referred to as zeolitic imidazolate frameworks (ZIFs).^[24,25] ZIFs containing two different imidazole linkers exhibited higher CO_2/CO selectivities compared to single-component ZIFs or the ternary MOF-5 derivatives.^[26] These MOFs of increasingly complex composition will inspire significant future challenges of rationally predicting the properties of binary, ternary, and higher order frameworks, given that the number of possible materials increases exponentially with the number of building blocks. It will also be important to measure the reactivity ratios of each monomer, as Yaghi and co-workers showed that the composition of several of their binary MOFs did not reflect the monomer feed ratios. Disparate rates of nucleation and incorporation could produce individual crystals with varying local compositions or the formation of single-monomer domains.

Jiang and co-workers used an IML approach to functionalize the pores of 2D COFs.^[27] Benzyl azide moieties were incorporated into the pores of the known HHTP-BDBA (COF-5) and NiPc-BDBA COF (Figure 2b) lattices by modifying the diboronic acid building block **8**. The amount of azide incorporated into each material was varied by changing the $[\mathbf{8}]:[\text{BDBA}]$ feed ratio. After COF formation, the azide groups were transformed into 1,4-triazoles using the Cu-catalyzed azide-alkyne cycloaddition (CuAAC) reaction, a transformation previously used to functionalize alkyne-containing MOFs. The efficiency of the CuAAC reaction was characterized through the disappearance of the azide stretch using FTIR spectroscopy when large excesses of the alkynes (>80 equivalents per azide) were employed. A reduced $S_{\text{BET}}\text{-N}_2$ was observed as a consequence of filling the pores with new functionality. These results indicate that postsynthetic functionalization of COFs can be performed in a similar fashion to MOFs,^[28] offering a means to engineer the pores of this emerging class of materials.

As is evident from the above examples, the IML approach is an intuitive and well-established method to modify framework properties and incorporate additional functionality into the pores. Its key advantage is that the framework topology is retained^[29] as the structures and relative ratios of

the monomers are varied. Nevertheless, the structures of IML-derived materials are less defined than their corresponding single-component networks and offer additional challenges in their characterization. Many existing reports assume that the building blocks are randomly mixed throughout the materials, but differences in reactivity or compatibility between monomers, as observed in some of the above studies, might lead to heterogeneous distributions, such as radial gradients, core-shell architectures, or even segregation into single-component domains. Each of these phenomena is an intriguing possibility and should be considered when evaluating new systems. Characterizing the precise locations of each monomer is challenging in most cases and might benefit from advances in spectroscopy. On the bulk scale, TGA can infer and quantify the presence of phase impurities, but diagnostic bimodal differential mass loss curves have also been observed for imidazolate-linked MOFs (ZIFs) with monodisperse pore-size distributions.^[25] Single-crystal X-ray diffraction is a powerful tool for atomic-scale characterization, but is unable to resolve the nonperiodic arrangements of multiple monomers throughout the framework. In one notable example, the two isostructural linkers used to make a series of imidazolate-linked MOFs occupied crystallographically distinct sites, allowing for their exact locations to be identified.^[30] Yaghi and co-workers also demonstrated homogeneous distribution over $100 \mu\text{m}$ length scale by dividing large single crystals of two-component MOF-5 derivatives and analyzing their composition.^[23] Developing a molecular-level understanding, along with an improved ability to predict the properties of binary, ternary, and even higher order IML frameworks, will provide a rational means to explore the vast chemical space available through the IML strategy. Mixing isostructural linkers has proven to be a simple and effective way to enhance framework properties and enabled the synthesis of COFs with tunable functionality. The stage is now set for using mixed-composition networks, combined with modular pore-functionalization strategies, to obtain otherwise inaccessible high-performance porous materials.

Heterostructural Mixed Linker Approaches

Though less intuitive than the IML strategy, mixing building blocks with different coordination geometries, denoted as a heterostructural mixed linker (HML) approach, provides opportunities to functionalize existing frameworks and to access lower symmetry topologies with large pore sizes. First demonstrated in MOF synthesis in 2003,^[31] HML topologies show a strong dependence on the monomer feed ratio and linker length, resulting in reduced predictability over network topology that complicates rational design. Contemporary studies continue to explore the design criteria for HML MOFs while optimizing their promising framework properties.

Matzger and co-workers performed the first rigorous study of a MOF derived from the HML strategy, in which **1**

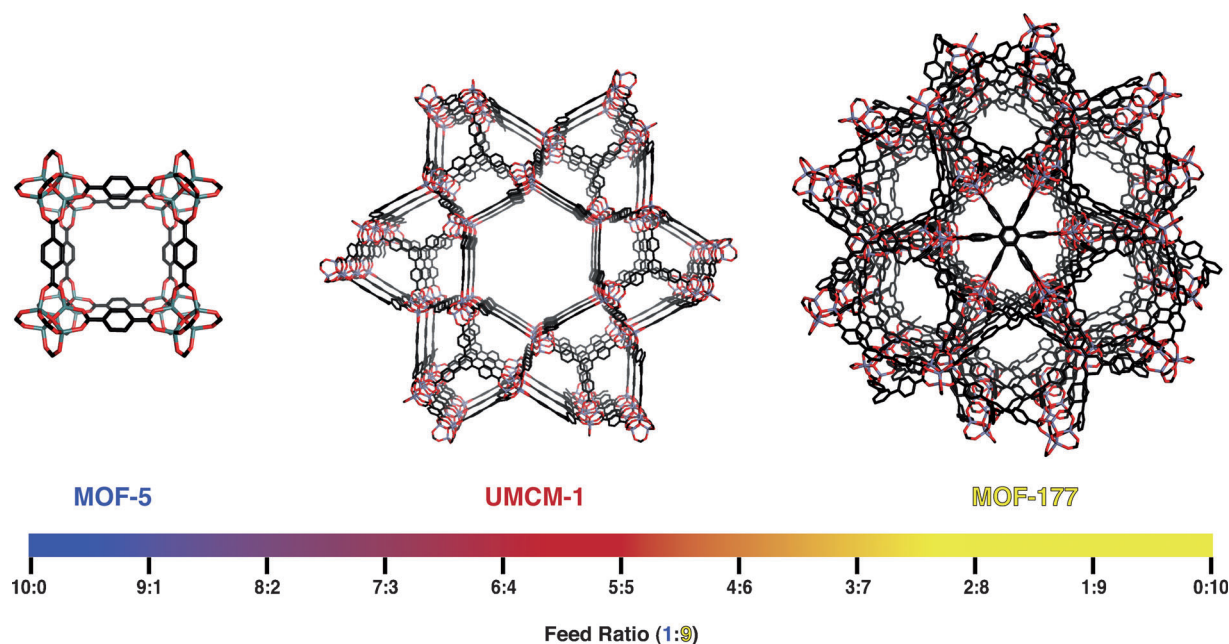


Figure 4. Phase diagram for UMCM-1 synthesis.

and a trifunctional carboxylic acid (**9**) were cocrystallized in the presence of $\text{Zn}(\text{NO}_3)_2$.^[32] On their own, **1** produces MOF-5, and **9** produces MOF-177 (Figure 4). Cocrystallization of the two linkers produces a new MOF (UMCM-1) containing 3.1 nm mesoporous hexagonal channels surrounded by 1.4 nm microporous cages. Mesoporous crystalline networks are less common than their microporous counterparts, because they are susceptible to pore collapse or interpenetration. Avoiding these phenomena is crucial for achieving high H_2 storage capacities.^[33] The HML approach, along with other strategies to desymmetrize MOF building blocks,^[34] show great promise in this area. UMCM-1 is non-interpenetrated and retains its high surface area ($4160 \text{ m}^2 \text{ g}^{-1}$) even after heating at 300°C for 3 h. Its formation is notably dependent on the building block feed ratio, crystallizing exclusively at ratios between 3:2 and 1:1 of **1:9**. Outside of this range, excess **1** produced either MOF-5 loaded with **9** occupying defect sites or physical mixtures of the two MOFs. Similarly, excess **9** produced either MOF-177 containing small amounts of **1** or mixtures of MOF-177 and UMCM-1 (Figure 4).

Interestingly, the phase window for forming UMCM-1 does not correspond to its 1:1.33 ratio of **1:9** found in the framework. The authors rationalized this finding by calculating the probability of the possible coordination modes of the two linkers to the Zn_4O secondary building unit (SBU). This study suggested that the maximum probability of forming the SBU coordination geometry found in UMCM-1 matched the feed ratios that yielded it in phase-pure form. This model offers a first step towards rational design of HML frameworks and highlights the open question of which factors influence their growth. Once conditions likely to pro-

duce phase-pure materials were identified, other linear dicarboxylates were used in place of **1** to provide other HML MOF topologies (Figure 5).^[35] It is thought that the relative sizes of the two linkers influence which of these networks are formed. These topological differences have important consequences for guest uptake and release, as illustrated by the vastly different diffusion behaviors observed in a single-molecule study of diffusion within the pores of UMCM-1, -2, and -4.^[36]

UMCM-2 is synthesized from mixtures of **9** and benzodithiophene (**10**) and adopts a similar structure to UMCM-1, with microporous cages surrounding a central micropore, but the central micropore is blocked by the trifunctional linker and is surrounded by two distinct microporous cages.^[37] UMCM-2 exhibits an exceptionally high BET surface area ($5200 \text{ m}^2 \text{ g}^{-1}$). Interestingly, improvement in H_2 storage capacity (6.9 wt% at 77 K and 46 bar) is not commensurate with its exceptional surface area. Subsequent studies on UMCM-1 revealed the H_2 storage capacity to be 6.23 wt% at 77 K and 20 bar, which was predicted to be as high as 9.5 wt% at elevated pressure (100 bar).^[38]

The increased pore size in UMCM-1 has also been exploited for postsynthetic modification. Cohen and co-workers synthesized an amine-functionalized UMCM-1 derivative (UMCM-1-NH₂) by replacing **1** with **2**.^[39,40] Acylation of the amines in the pores of UMCM-1-NH₂ with increasingly bulky carboxylic acid anhydrides indicated that its larger pores accommodated longer alkyl chains relative to amines located within cubic MOFs.^[39] Cohen and co-workers subsequently demonstrated that terminal olefins introduced into UMCM-1-NH₂ undergo Diels–Alder cycloadditions with an s-tetrazine.^[40] UMCM-1-NH₂ was also condensed with 2-for-

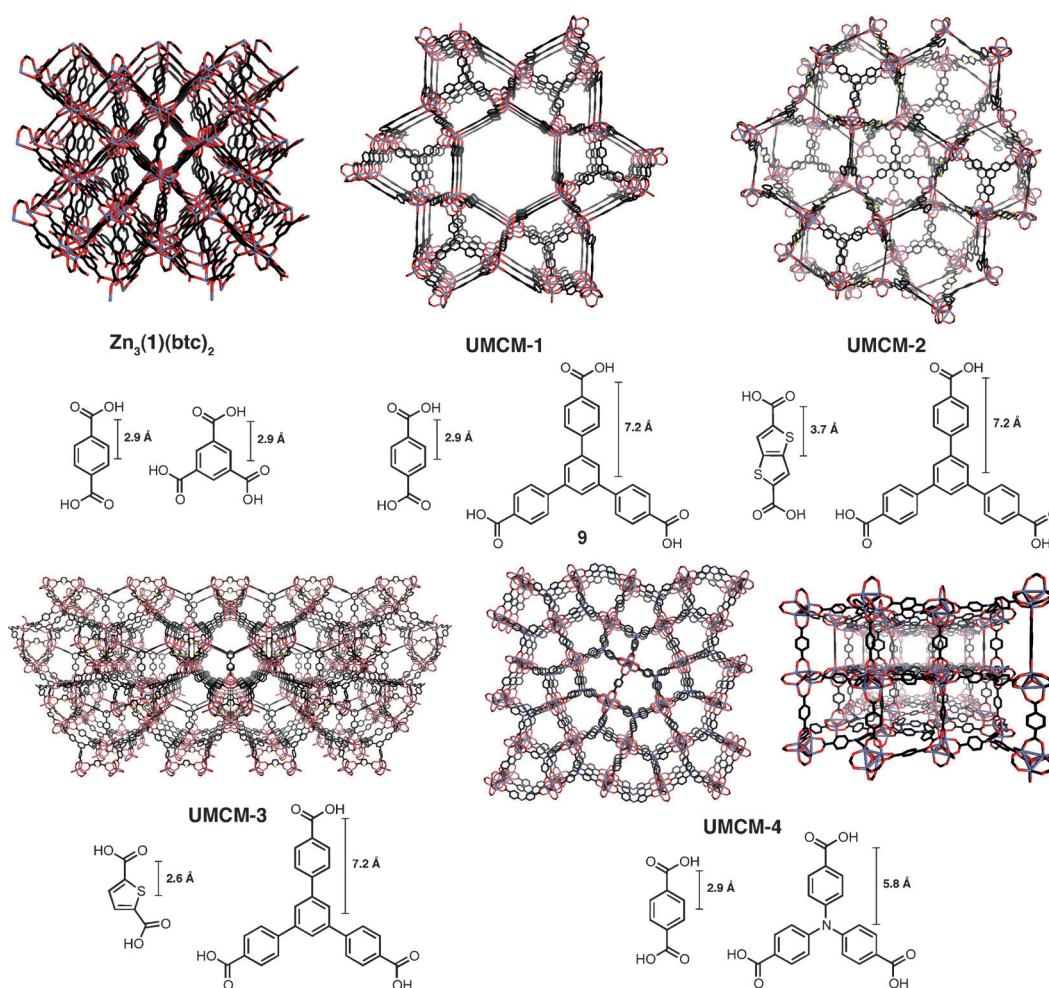


Figure 5. Small variations of relative linker lengths of mixtures of di- and trifunctional linkers dramatically affect the topologies of HML MOFs.

mylpyridine, providing a chelate for Pd^{2+} ions, although its catalytic properties were not investigated.^[41] Kaskel and co-workers condensed a terephthalic acid derivative bearing a S-oxazolidinone to yield optically active UMCM-1.^[42] When employed as an HPLC stationary phase, this MOF separated enantiomers of 1-phenylethanol with a moderate but unoptimized selectivity factor (α) of 1.6 and resolution (R_s) of 0.65. The wide variety of potential functional groups that might be incorporated into its large pores make UMCM-1 derivatives promising from the standpoint of framework integrity and internal accessibility. Elsewhere on the UMCM-1 phase diagram, Matzger and co-workers noted the presence of phase-pure MOF-5 containing **9** within the crystal.^[43] Trifunctional carboxylic acid **9** is presumed to occupy defect sites within the lattice, leaving free carboxylic acids within the pores. Exposing this framework to $\text{Pd}(\text{OAc})_2$ yields Pd^{2+} -functionalized materials capable of catalyzing C–H activation. Interestingly, the regioselectivity for the arylation of naphthalene changed from 1-phenylnaphthalene to 2-phenylnaphthalene when using the MOF catalyst as compared to dissolved $\text{Pd}(\text{OAc})_2$.

As shown from the examples above, the HML strategy provides access to unavailable topologies and larger pore sizes not easily achieved in single-component frameworks. These desirable properties come at the expense of the predictability of the network topology. Small changes in both the di- and trifunctional linker sizes induce significant topological differences, directly impacting framework properties. Existing frameworks were rationalized empirically and great opportunity lies in the ability to predict topologies and phase windows in HML systems.

Truncated Mixed Linker Approaches

A third strategy to obtain multicomponent frameworks employs a truncated mixed-linker (TML) approach, in which a polyfunctional monomer is cocondensed with a monomer bearing fewer reactive groups. The relative rates of bond formation and exchange dictate the role of the truncated monomer in the crystallization. If growth is faster than exchange, the truncated monomer is incorporated throughout

the network, which grows around these defect sites. If exchange is rapid relative to framework growth, the truncated monomer will preferentially reside at the faces of the growing crystal, providing a means to control its size, shape, and surface functionality.

Operating in the slow exchange regime, we recently utilized the TML strategy to functionalize the interior of a boroxine-linked 3D COF (COF-102) derived from the dehydration of tetrakis(boronic acid) **11**.^[44] A second monomer, incorporating either a *n*-dodecyl ($-C_{12}H_{25}$) or allyl group in place of one phenylboronic acid moiety, was included in the crystallization (Figure 6). The rate of incorporation of the dodecyl-truncated comonomer into the framework scaled with the feed ratio and the resulting frameworks were essentially indistinguishable from pristine COF-102 by scanning electron microscopy (SEM) and powder X-ray diffraction (PXRD). The $S_{\text{BET-N}_2}$ and pore volume of the functionalized materials were inversely proportional to dodecyl loading, consistent with the alkyl chains occupying the interior pore volume. The presence of the truncated monomer within the framework was supported by a TEM study in which crystallites of allyl-functionalized COF-102 were stained with OsO_4 and microtomed, revealing the presence of Os within their interior. Loadings of up to 33% truncated monomer were observed, offering an opportunity for facile loading of these high surface area materials with large amounts of payload.

The Kitagawa group used the TML strategy under faster exchange conditions to grow microporous nanorods of the $\text{Cu}_2(\mathbf{12})(\text{dabco})$ framework, which has carboxylate-Cu coordination oriented in the [100] direction and N-Cu coordination in the [001] orientation (Figure 7).^[45] Including acetic acid during the crystallization results in competitive coordination with **12**, thus slowing growth in the [100] direction. Growth in the [001] direction remains uninhibited, yielding anisotropic nanorods. A study of the crystallization process using TEM revealed nanoparticle formation at short growth times, which aggregate into cubic structures that grew selectively in the [001] direction.

The Kitagawa group subsequently demonstrated similar morphological control in MOFs linked exclusively by metal-carboxylate coordination.^[46] Increasing concentrations of lauric acid included in a prenucleation step with $\text{Cu}(\text{NO}_3)_2$, followed by subsequent framework growth with benzenetri-

(carboxylic acid) (btc), provided the $\text{Cu}_3(\text{btc})_2$ framework with varying crystallite morphologies. These morphologies changed from octahedral to cuboctahedral to cubic as the lauric acid concentration was increased. Monte-Carlo simulations of a coarse grain model of this framework suggested that the observed morphologies were consistent with the lauric acid preferentially inhibiting growth at the [100] face. Prenucleation and subsequent framework growth also yielded oriented cuboctahedral and cubic crystallites on bare Au substrates, representing a straightforward protocol for orienting MOFs through crystal engineering strategies.

Yaghi and co-workers applied a similar TML approach to the cubic MOF-5 structure, whose symmetry precludes selective directional growth.^[47] In this case, MOF-5 crystallizes in the presence of varying amounts of a dodecyloxybenzoic acid and yields macroporous crystallites that retain the cubic framework structure, a morphology reminiscent of Swiss cheese. Interestingly, digested solutions of these materials did not contain the dodecyloxybenzoic acid, suggesting that it was washed out of the macroporous structures during isolation or activation. This change in crystallite morphology was associated with a reduced Langmuir surface area as measured by N_2 adsorption, yet these samples showed increased capacity for CO_2 .

The TML approach operates across a broad continuum of exchange and error correction rates, providing outcomes ranging from internal functionalization to anisotropic crystallization. These results also highlight the unanswered question of what reaction and exchange rates are required for framework formation. COF-102 growth occurred too rapidly for truncated monomers to be removed through boroxine exchange reactions, demonstrating that rapid exchange is not necessary for framework crystallization. Faster exchange enabled engineering of the size and shape of MOF crystallites, allowing specific morphologies to be targeted. Currently, reaction exchange rates are uncontrolled and often rationalized empirically after framework synthesis. An improved understanding of the kinetics of exchange as it relates to framework growth will provide fundamental insight into reliably applying the TML strategy. This strategy also parallels the field of molecular capsules, in which all linkers are truncated. In 1990, Fujita first employed an intuitive design approach whereby a metal vertex and organic linker predictably formed a square-shaped macrocycle following funda-

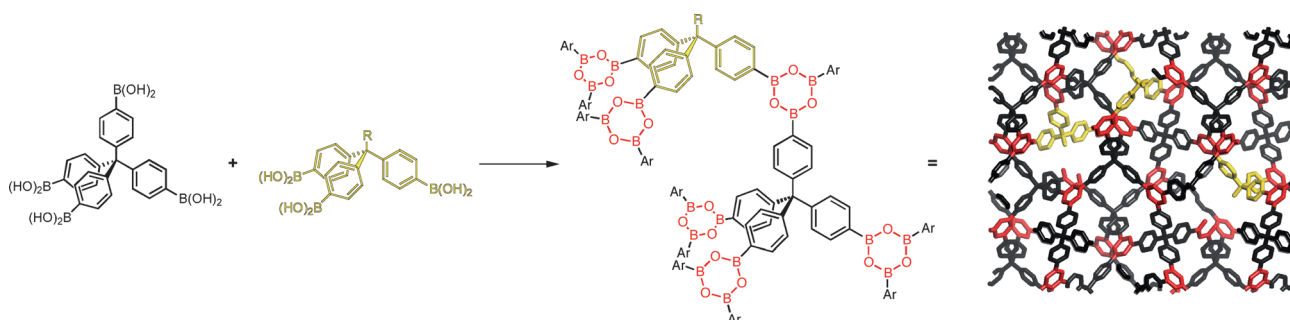


Figure 6. Truncated monomers included in COF-102 crystallization yield functionalized frameworks.

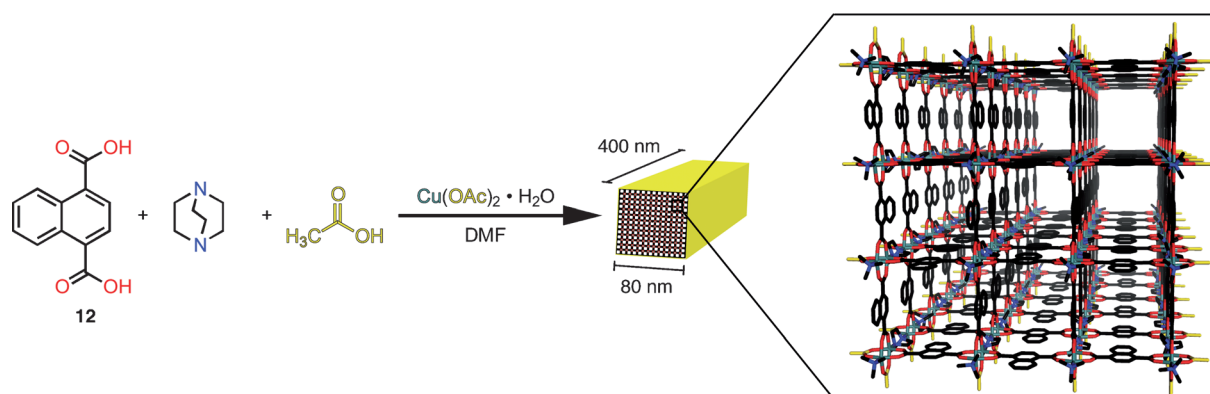


Figure 7. Acetic acid mediates the growth of the [100] face of $\text{Cu}_2(\mathbf{12})(\text{dabco})$, favoring nanorod growth in the [001] direction.

mental geometric principles.^[48] This directional bonding approach, which predates all but the earliest three-dimensional coordination networks,^[49] has since been applied to a wide range of 2D and 3D structures.^[50] Knowledge gained in this field over the past two decades serves as a basis for understanding the related chemistry involved in TML framework synthesis. Further investigation into the kinetics of crystallization using the TML strategy will elucidate the role of the truncating agent, enabling reliable crystal engineering or framework functionalization as dictated by the specific application.

Outlook

The three mixed linker strategies highlighted in this Concept Article enable the synthesis of functionalized topologies and underline their potential use in separations, payload storage and release, and catalysis. The focus of the framework materials field is now broadening beyond established applications, such that designing functional platforms whose properties can be tuned modularly is increasingly important. Moving from empirical to rational design remains an outstanding challenge among each of the mixed linker strategies. Predicting emerging properties (via IML), framework topologies (via HML), and crystallization kinetics (via TML) represent important frontiers for which improved understanding will enhance framework utility. These strategies will also provide a means to optimize many framework properties, including gas sorption, loading/release kinetics, and improvements in catalytic performance.

Acknowledgements

Our research on framework materials has been generously supported by Cornell University, the NSF CAREER award (CHE-1056657), the Sloan Research Fellowship, the Cottrell Scholar Award from Research Corporation for Science Advancement, and a 3M Nontenured Faculty Award. D.N.B. acknowledges the award of a Graduate Research Fellowship from the NSF.

- [1] J. R. Long, O. M. Yaghi, *Chem. Soc. Rev.* **2009**, *38*, 1213.
- [2] D. J. Tranchemontagne, J. L. Mendoza-Cortés, M. O’Keeffe, O. M. Yaghi, *Chem. Soc. Rev.* **2009**, *38*, 1257.
- [3] a) X. Feng, X. Ding, D. Jiang, *Chem. Soc. Rev.* **2012**, *41*, 6010; b) A. P. Côté, A. I. Benin, N. W. Ockwig, A. J. Matzger, M. O’Keeffe, O. M. Yaghi, *Science* **2005**, *310*, 1166.
- [4] H. M. El-Kaderi, J. R. Hunt, J. L. Mendoza-Cortés, A. P. Côté, R. E. Taylor, M. O’Keeffe, O. M. Yaghi, *Science* **2007**, *316*, 268.
- [5] a) E. L. Spitler, W. R. Dichtel, *Nat. Chem.* **2010**, *2*, 672; b) E. L. Spitler, M. R. Giovino, S. L. White, W. R. Dichtel, *Chem. Sci.* **2011**, *2*, 1588; c) E. L. Spitler, B. T. Koo, J. L. Novotney, J. W. Colson, F. J. Uribe-Romo, G. D. Gutierrez, P. Clancy, W. R. Dichtel, *J. Am. Chem. Soc.* **2011**, *133*, 19416; d) R. W. Tilford, W. R. Gemmill, H.-C. zur Loye, J. J. Lavigne, *Chem. Mater.* **2006**, *18*, 5296; e) E. L. Spitler, J. W. Colson, F. J. Uribe-Romo, A. R. Woll, M. R. Giovino, A. Saldivar, W. R. Dichtel, *Angew. Chem.* **2012**, *124*, 2677; *Angew. Chem. Int. Ed.* **2012**, *51*, 2623.
- [6] a) S.-Y. Ding, J. Gao, Q. Wang, Y. Zhang, W.-G. Song, C.-Y. Su, W. Wang, *J. Am. Chem. Soc.* **2011**, *133*, 19816; b) F. J. Uribe-Romo, J. R. Hunt, H. Furukawa, C. Klöck, M. O’Keeffe, O. M. Yaghi, *J. Am. Chem. Soc.* **2009**, *131*, 4570.
- [7] F. J. Uribe-Romo, C. J. Doonan, H. Furukawa, K. Oisaki, O. M. Yaghi, *J. Am. Chem. Soc.* **2011**, *133*, 11478.
- [8] a) J. W. Colson, A. R. Woll, A. Mukherjee, M. P. Levendorf, E. L. Spitler, V. B. Shields, M. G. Spencer, J. Park, W. R. Dichtel, *Science* **2011**, *332*, 228; b) S. Wan, J. Guo, J. Kim, H. Ihee, D. Jiang, *Angew. Chem.* **2008**, *120*, 8958; *Angew. Chem. Int. Ed.* **2008**, *47*, 8826; c) S. Wan, J. Guo, J. Kim, H. Ihee, D. Jiang, *Angew. Chem.* **2009**, *121*, 5547; *Angew. Chem. Int. Ed.* **2009**, *48*, 5439.
- [9] H. Furukawa, O. M. Yaghi, *J. Am. Chem. Soc.* **2009**, *131*, 8875.
- [10] A. D. Burrows, *CrystEngComm* **2011**, *13*, 3623.
- [11] A. D. Burrows, C. G. Frost, M. F. Mahon, C. Richardson, *Angew. Chem.* **2008**, *120*, 8610; *Angew. Chem. Int. Ed.* **2008**, *47*, 8482.
- [12] H. Chun, D. N. Dybtsev, H. Kim, K. Kim, *Chem. Eur. J.* **2005**, *11*, 3521.
- [13] T. Fukushima, S. Horike, Y. Inubushi, K. Nakagawa, Y. Kubota, M. Takata, S. Kitagawa, *Angew. Chem.* **2010**, *122*, 4930; *Angew. Chem. Int. Ed.* **2010**, *49*, 4820.
- [14] A. D. Burrows, L. C. Fisher, C. Richardson, S. P. Rigby, *Chem. Commun.* **2011**, *47*, 3380.
- [15] S. Marx, W. Kleist, J. Huang, M. Maciejewski, A. Baiker, *Dalton Trans.* **2010**, *39*, 3795.
- [16] a) Y. Huang, S. Gao, T. Liu, J. Lü, X. Lin, H. Li, R. Cao, *ChemPlusChem* **2012**, *77*, 106; b) T. Lescouet, E. Kockrick, G. Bergeret, M. Pera-Titus, S. Aguado, D. Farrusseng, *J. Mater. Chem.* **2012**, *22*, 10287.
- [17] K. M. L. Taylor-Pashow, J. D. Rocca, Z. Xie, S. Tran, W. Lin, *J. Am. Chem. Soc.* **2009**, *131*, 14261.

- [18] W. Kleist, F. Jutz, M. Maciejewski, A. Baiker, *Eur. J. Inorg. Chem.* **2009**, 3552.
- [19] W. Kleist, M. Maciejewski, A. Baiker, *Thermochim. Acta* **2010**, *499*, 71.
- [20] M. Kim, J. F. Cahill, K. A. Prather, S. M. Cohen, *Chem. Commun.* **2011**, *47*, 7629.
- [21] a) M. Kim, J. F. Cahill, Y. Su, K. A. Prather, S. M. Cohen, *Chem. Sci.* **2012**, *3*, 126; b) M. Kim, J. F. Cahill, H. Fei, K. A. Prather, S. M. Cohen, *J. Am. Chem. Soc.* **2012**, *134*, 18082.
- [22] T.-H. Park, K. Koh, A. G. Wong-Foy, A. J. Matzger, *Cryst. Growth Des.* **2011**, *11*, 2059.
- [23] H. Deng, C. J. Doonan, H. Furukawa, R. B. Ferreira, J. Towne, C. B. Knobler, B. Wang, O. M. Yaghi, *Science* **2010**, *327*, 846.
- [24] a) J. Kahr, J. P. S. Mowat, A. M. Z. Slawin, R. E. Morris, D. Fairen-Jimenez, P. A. Wright, *Chem. Commun.* **2012**, *48*, 6690; b) S. Bernt, M. Feyand, A. Modrow, J. Wack, J. Senker, N. Stock, *Eur. J. Inorg. Chem.* **2011**, 5378.
- [25] J. A. Thompson, C. R. Blad, N. A. Brunelli, M. E. Lydon, R. P. Lively, C. W. Jones, S. Nair, *Chem. Mater.* **2012**, *24*, 1930.
- [26] R. Banerjee, A. Phan, B. Wang, C. Knobler, H. Furukawa, M. O'Keeffe, O. M. Yaghi, *Science* **2008**, *319*, 939.
- [27] A. Nagai, Z. Guo, X. Feng, S. Jin, X. Chen, X. Ding, D. Jiang, *Nat. Commun.* **2011**, *2*, 536.
- [28] a) S. M. Cohen, *Chem. Rev.* **2012**, *112*, 970; K. K. Tanabe, S. M. Cohen, *Chem. Soc. Rev.* **2011**, *40*, 498; b) T. Gadzikwa, O. K. Farha, C. D. Malliakas, M. G. Kanatzidis, J. T. Hupp, S. T. Nguyen, *J. Am. Chem. Soc.* **2009**, *131*, 13613.
- [29] For a recent IML example using two monomers of different lengths to obtain new topologies, see K. Koh, J. D. Van Oosterhout, S. Roy, A. G. Wong-Foy, A. J. Matzger, *Chem. Sci.* **2012**, *3*, 2429.
- [30] R. Banerjee, H. Furukawa, D. Britt, C. Knobler, M. O'Keeffe, O. M. Yaghi, *J. Am. Chem. Soc.* **2009**, *131*, 3875.
- [31] W. Chen, J.-Y. Wang, C. Chen, Q. Yue, H.-M. Yuan, J.-S. Chen, S.-N. Wang, *Inorg. Chem.* **2003**, *42*, 944.
- [32] K. Koh, A. G. Wong-Foy, A. J. Matzger, *Angew. Chem.* **2008**, *120*, 689; *Angew. Chem. Int. Ed.* **2008**, *47*, 677.
- [33] H. Frost, R. Q. Snurr, *J. Phys. Chem. C* **2007**, *111*, 18794; L. J. Murray, M. Dincă, J. R. Long, *Chem. Soc. Rev.* **2009**, *38*, 1294.
- [34] a) F. Nouar, J. F. Eubank, T. Bousquet, L. Wojtas, M. J. Zaworotko, M. Eddaoudi, *J. Am. Chem. Soc.* **2008**, *130*, 1833; b) O. K. Farha, C. E. Wilmer, I. Eryazici, B. G. Hauser, P. A. Parilla, K. O'Neill, A. A. Sarjeant, S. T. Nguyen, R. Q. Snurr, J. T. Hupp, *J. Am. Chem. Soc.* **2012**, *134*, 9860.
- [35] K. Koh, A. G. Wong-Foy, A. J. Matzger, *J. Am. Chem. Soc.* **2010**, *132*, 15005.
- [36] Y. Liao, S. K. Yang, K. Koh, A. J. Matzger, J. S. Biteen, *Nano Lett.* **2012**, *12*, 3080.
- [37] K. Koh, A. G. Wong-Foy, A. J. Matzger, *J. Am. Chem. Soc.* **2009**, *131*, 4184.
- [38] a) B. Mu, P. M. Schoenecker, K. S. Walton, *J. Phys. Chem. C* **2010**, *114*, 6464; b) Z. Xiang, J. Lan, D. Cao, X. Shao, W. Wang, D. P. Broom, *J. Phys. Chem. C* **2009**, *113*, 15106.
- [39] Z. Wang, K. K. Tanabe, S. M. Cohen, *Inorg. Chem.* **2009**, *48*, 296.
- [40] C. Chen, C. A. Allen, S. M. Cohen, *Inorg. Chem.* **2011**, *50*, 10534.
- [41] C. J. Doonan, W. Morris, H. Furukawa, O. M. Yaghi, *J. Am. Chem. Soc.* **2009**, *131*, 9492.
- [42] M. Padmanaban, P. Muller, C. Lieder, K. Gedrich, R. Grunker, V. Bon, I. Senkovska, S. Baumgartner, S. Opelt, S. Paasch, E. Brunner, F. Glorius, E. Klemm, S. Kaskel, *Chem. Commun.* **2011**, *47*, 12089.
- [43] T.-H. Park, A. J. Hickman, K. Koh, S. Martin, A. G. Wong-Foy, M. S. Sanford, A. J. Matzger, *J. Am. Chem. Soc.* **2011**, *133*, 20138.
- [44] D. N. Bunck, W. R. Dichtel, *Angew. Chem. Int. Ed.* **2012**, *51*, 1885.
- [45] T. Tsuruoka, S. Furukawa, Y. Takashima, K. Yoshida, S. Isoda, S. Kitagawa, *Angew. Chem.* **2009**, *121*, 4833; *Angew. Chem. Int. Ed.* **2009**, *48*, 4739.
- [46] A. Umemura, S. Diring, S. Furukawa, H. Uehara, T. Tsuruoka, S. Kitagawa, *J. Am. Chem. Soc.* **2011**, *133*, 15506.
- [47] K. M. Choi, H. J. Jeon, J. K. Kang, O. M. Yaghi, *J. Am. Chem. Soc.* **2011**, *133*, 11920.
- [48] M. Fujita, J. Yazaki, K. Ogura, *J. Am. Chem. Soc.* **1990**, *112*, 5645.
- [49] B. F. Hoskins, R. Robson, *J. Am. Chem. Soc.* **1989**, *111*, 5962.
- [50] a) R. Chakrabarty, P. S. Mukherjee, P. J. Stang, *Chem. Rev.* **2011**, *111*, 6810; b) D. J. Tranchemontagne, Z. Ni, M. O'Keeffe, O. M. Yaghi, *Angew. Chem.* **2008**, *120*, 5214; *Angew. Chem. Int. Ed.* **2008**, *47*, 5136.

Received: September 5, 2012
Published online: December 27, 2012